

Received: 2015.04.09
Accepted: 2015.04.09
Published: 2015.07.27

Evaluation of Vibration Response Imaging (VRI) Technique and Difference in VRI Indices Among Non-Smokers, Active Smokers, and Passive Smokers

Authors' Contribution:
Study Design A
Data Collection B
Statistical Analysis C
Data Interpretation D
Manuscript Preparation E
Literature Search F
Funds Collection G

ABCDEF G 1,2 **Hongying Jiang***
ABCDEF 1,2 **Jichao Chen***
BCD 1,2 **Jinying Cao**
BDF 1,2 **Lan Mu**
BDE 1,2 **Zhenyu Hu**
CDF 1,2 **Jian He**

1 Department of Respiratory Medicine, Aerospace Center Hospital, Beijing, P.R. China
2 Aerospace Clinical Medical College of Peking University, Peking University, Beijing, P.R. China

* These authors contributed to equally to this work

Corresponding Author: Hongying Jiang, e-mail: Jiang042948954@126.com

Source of support: This work was supported by the Medical and Health Research Projects of the China Aerospace Science and Industry Group, LTD (JKBZ-001)

Background: Vibration response imaging (VRI) is a new technology for lung imaging. Active smokers and non-smokers show differences in VRI findings, but no data are available for passive smokers. The aim of this study was to evaluate the use of VRI and to assess the differences in VRI findings among non-smokers, active smokers, and passive smokers.





Material/Methods: Healthy subjects (n=165: 63 non-smokers, 56 active smokers, and 46 passive smokers) with normal lung function were enrolled. Medical history, physical examination, lung function test, and VRI were performed for all subjects. Correlation between smoking index and VRI scores (VRIS) were performed.

Results: VRI images showed progressive and regressive stages representing the inspiratory and expiratory phases bilaterally in a vertical and synchronized manner in non-smokers. Vibration energy curves with low expiratory phase and plateau were present in 6.35% and 3.17%, respectively, of healthy non-smokers, 41.07% and 28.60% of smokers, and 39.13% and 30.43% of passive smokers, respectively. The massive energy peak in the non-smokers, smokers, and passive-smokers was 1.77 ± 0.27 , 1.57 ± 0.29 , and 1.66 ± 0.33 , respectively (all $P < 0.001$). A weak but positive correlation was observed between VRIS and smoking index.

Conclusions: VRI can intuitively show the differences between non-smokers and smokers. VRI revealed that passive smoking can also harm the lungs. VRI could be used to visually persuade smokers to give up smoking.

MeSH Keywords: **Hand-Arm Vibration Syndrome • Hydrothermal Vents • Imaging, Three-Dimensional**

Full-text PDF: <http://www.medscimonit.com/abstract/index/idArt/894335>

 2822  3  7  23



Background

Vibration response imaging (VRI) is a non-invasive, radiation-free imaging device that uses the vibration energy of the sound created by the lungs during breathing [1]. The device creates a dynamic image of the lungs using an array of active sensors [1,2]. VRI has sparked a great deal of interest in a wide range of clinical and research settings related to respiratory care and medicine [1,3].

Previous studies have demonstrated the advantages of VRI in the diagnosis and follow-up of many respiratory diseases [3–5]. Lung sounds can be visually characterized in healthy individuals using VRI [4,5]. It was found that the images from subjects with respiratory illness differed substantially from the images of the healthy subjects [1]. In another study, respiratory sounds from patients with dyspnea due to obstructive airway disease (OAD) and those with dyspnea not due to OAD were compared with normal controls using VRI, and it was found that the ratios of peak inspiratory to peak expiratory vibration energy was significantly lower in the dyspnea group compared with normal controls [3]. In addition, VRI was used to detect and quantify pleural effusions [2].

Two previous studies compared the VRI findings between active smokers and non-smokers, and showed that smokers were more likely to display changes in VRI findings [6,7]. However, no data is yet available about passive smokers. Therefore, the present study aimed to evaluate the use of VRI and describe the differences in VRI findings between non-smokers, active smokers and passive smokers.

Material and Methods

Subjects

This was a prospective cohort study carried out between February 2012 and September 2012 at the Aerospace Center Hospital, Aerospace Clinical Medical College of Peking University, Beijing, China. Inclusion criteria were: 1) men and women older than 18 years; 2) able to read and understand the informed consent independently; 3) absence of chronic respiratory disease or cardiovascular disease or negative history of respiratory infection in the previous month; 4) normal X-ray and physical examinations; and 5) normal lung function ($FEV_1/FVC > 70\%$, $FEV_1/FEV_1 \text{ Pred} > 80\%$, and $FVC/FVC \text{ Pred} > 80\%$, where FEV_1 is the forced expiratory volume in one second and FVC is the forced vital capacity). Exclusion criteria were: 1) severe deformity of thorax or spinal column, skin injury on the back, or acute respiratory infection; 2) presence of a pacemaker implant or defibrillator; or 3) pregnant or lactating women.



Figure 1. Vibration response imaging device. The photograph shows the placement and attachment of the planar arrays on the subject's back using gentle suction. Each planar array is composed of six rows of three sensors.

Active smoking refers to persons who smoked consecutively or accumulatively for at least six months during their lifetime. Passive smokers refer to non-smoking persons who are exposed to secondary smoke by means of smoke from a lit cigarette or smoke breathed out from smokers for at least 15 minutes in a day per week [8]. The smoking index was determined as the number of packs of cigarettes smoked per day multiplied by the number of smoking years [9].

This study was approved by the Institutional Review Board and Ethical Committee of Aerospace Center Hospital, Aerospace Clinical Medical College of Peking University, Beijing, China. The written informed consent was obtained from all subjects.

VRI device and procedure

The procedure was performed using the VRI device (VRIxp System, Deep Breeze Ltd, Or Akiva, Israel) in the sitting position. Two arrays of sensors (6 rows by 3 columns each) were placed on the back of the subjects. Each sensor was attached to the back of the subject using gentle suction, according to the manufacturer's instructions (Figure 1) [6,10]. During deep respiratory cycles, recordings were performed over a 12-second period at a breath rate of 15–20 per minute.

All images were recorded by the same skilled technician. The VRI mode of presentation is a dynamic gray-scale digital image depicting the instantaneous acoustic energy derived from a series of frames. The frame obtained at peak inspiration

displays the distribution of the maximal vibration energy during the respiratory cycle, and is identified as the maximum energy frame (MEF). The gray-scale level depicts areas with high vibration energy as black, and areas with low vibration energy as light gray. The visual display is complemented by a quantitative lung data (QLD) distribution table of total vibration energy. For QLD, the VRIxp device acquires the signal data for all 12-second recordings, including both inspiration and expiration, and the algorithm extracts the relative intensity of breath sounds or vibrations for each lung and each lung region (upper, middle, and lower). Dry and moist rales are detected automatically by the VRI, and correspondingly marked as red and blue dots in the vibration energy figure.

VRI image analysis

Three trained readers who had received a systematic training performed a blinded image analysis independently. If there was disagreement, the final assessment was determined by consensus. Analysis of VRI images was performed based on the following aspects: 1) the overall shape and spatial distribution of the vibration energy curve; 2) the shape and area of the MEF; 3) dynamic image analysis (one by one observation from the first to the last frame); 4) QLD changes in different areas; 5) dry and moist rales; and 6) expiratory vibration energy peak (EVP), with focused observation on EVP synchronization (temporal synchronization of EVP between bilateral lungs) and EVP intensity (amplitude difference of EVP between bilateral lungs).

Image scores

VRI scores (VRIS) were calculated by adding up the following sub-scores. The maximal VRIS was 22 points [10–12].

(1) Vibration energy score (8 points): The normal vibration energy curve is smooth and continuous, like a double parabolic. The curve rises with inspiration, reaches the peak, and drops during the expiration phase. The abnormalities of vibration energy curve include dissimilar curves, plateau, sunken, spike, ladder, unidirectional curve, steep ladder inspiratory curve, and low-expiratory phase. The presence of each of these abnormalities scores 1 point, for a possible total of 8 points.

(2) MEF score (6 points): The MEF involves a video sequence that usually provides a great deal of information on the distribution of lung vibration and approximated peak inspiration. The normal MEF signs include smooth and equal energy distribution, with a vertical midline. The abnormal MEF signs include bulging, defect, roughness, asymmetry, midline bending, and several energy groups. The presence of each of these abnormalities scores one point, for a possible total of 6 points.

(3) Dynamic image score (8 points): Imaging progresses and regresses vertically and in a synchronized manner from top to bottom during both inspiration and expiration phases. Projections of right and left sides of images are the same as standard posteroanterior chest radiograph: the right side of the image displays the left lung. Right and left sides of the images develop simultaneously from early frames to the maximum energy frame. Image jumping includes a non-vibration type (0 point, the energy center has no quick change and discontinuous movement), a slight change (1 point, the movement of the energy occurs in 1-2 frame, occasionally at the inspiratory and expiratory phases), a moderate change (2 points, the movement of the energy occurs at the inspiratory or expiratory phase), and a severe change (3 points, the movement of the energy occurs at both the inspiratory and expiratory phases). Other abnormalities of dynamic imaging include dynamic image disorder, desynchronized development, delay, inverse dominance, and air trapping at the end of expiratory phase. The presence of each of these additional abnormalities scores one point, for a possible total of 5 points (or 8 for the entire sub-score).

Statistics analysis

SPSS 16.0 (IBM, Armonk, NY, USA) was used for statistical analysis. Continuous variables are presented as means \pm standard deviation (SD), and were compared between groups using analysis of variance method with the Tukey's post hoc test. Categorical data are presented as proportions, and were compared using the chi-square or the Fisher's exact test, as appropriate. Spearman's correlation analysis was used to compare the correlation between VRIS and smoking index. Two-sided P-values ≤ 0.05 were considered statistically significant.

Results

Subject characteristics

A total of 165 subjects were enrolled in this study (63 non-smokers, 56 smokers, and 46 passive smokers). Demographics, anthropometric values, and lung function test results of the study population are shown in Table 1. There was no difference in age, body mass index (BMI), or lung function between the 3 groups. However, there were more males in the active smoking group.

Adverse experience

All subjects underwent an uncomplicated recording procedure and no adverse events were reported during the study.

Table 1. Demographic characteristic, anthropometric values, and lung function test results of study population.

Characteristics	Non-smokers	Smokers	Passive smokers
No. of subjects	63	56	46
Age (y)	37.41±10.42	40.64±11.22	38.24±11.46
Sex (F,M)	40, 23	55, 1	27, 19
BMI (kg/m ²)	22.8±2.8	22.4±2.1	21.5±2.5
FEV ₁ /FVC	98.3±13.4	97.2±12.1	96.3±11.8
FEV ₁ /FEV ₁ Pred	106.2±13.7	99.8±13.8	104.2±12.7
FVC/FVC Pred	98.7±12.8	97.5±15.2	98.6±13.6

Values are presented as mean ±SD; FEV₁ – forced expiratory volume in one second; FVC – forced vital capacity.

Table 2. Vibration energy curve of smokers, passive smokers, and non-smokers.

Group	n	Low (%)	Platform (%)	Sunken (%)	Single peak (%)	Massive energy
Non-smokers	63	4 (6.35)	2 (3.17)	0 (0.00)	0 (0.00)	1.66±0.33
Smokers	56	23 (41.07)	16 (28.6)	2 (3.57)	3 (5.36)	1.77±0.27
Passive smokers	46	18 (39.13)	14 (30.43)	3 (6.52)	4 (9.00)	1.57±0.29
P		<0.001*	<0.001*	0.14	0.74	<0.001*

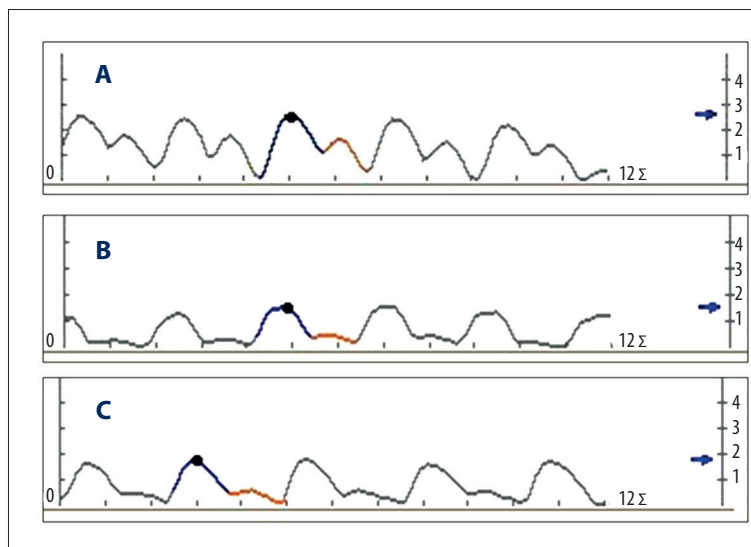


Figure 2. Comparison of vibration energy curves. The vibration energy curves of non-smokers (A), active smokers (B), and passive smokers (C). The x axis displays time (12 seconds). The y axis displays breathing intensity. The arrows indicate recordings of massive energy peak. The blue curve represents the inspiratory phase and red curve represents the expiratory phase. The vibration energy curve of non-smokers (A) was smooth, continuous, like a double parabolic. The curve rises with inspiration, reach a peak; when the curve drops, the expiration phase begin. The vibration energy curve of smokers and passive smokers (B, C) had a low expiratory phase and a plateau.

Vibration energy curve

Vibration energy curve with low-expiratory phase and plateau were present in 6.35% and 3.17%, respectively, of healthy non-smokers, 41.07% and 28.60% of smokers, and 39.13% and 30.43% of passive smokers. The massive energy peak in the non-smokers, smokers, and passive-smokers were 1.77±0.27, 1.57±0.29, and 1.66±0.33, respectively (Table 2, Figure 2).

MEF

No significant differences between non-smokers, smokers, and passive smokers were detected in the shape of missing parts of MEF ($P>0.05$) (Figure 3).

Dynamic image analysis

Significant differences in air trapping at the end of the expiratory phase were found between non-smokers, smokers,

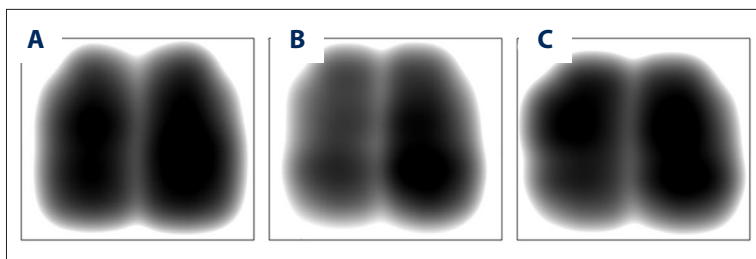


Figure 3. Comparison of MEF. MEF of non-smokers (A), active smokers (B), and passive smokers (C). The normal MEF looks like lungs, smooth, with equal energy distribution and the midline is vertical. There was no difference between non-smokers, smokers and passive smokers (P=0.575)

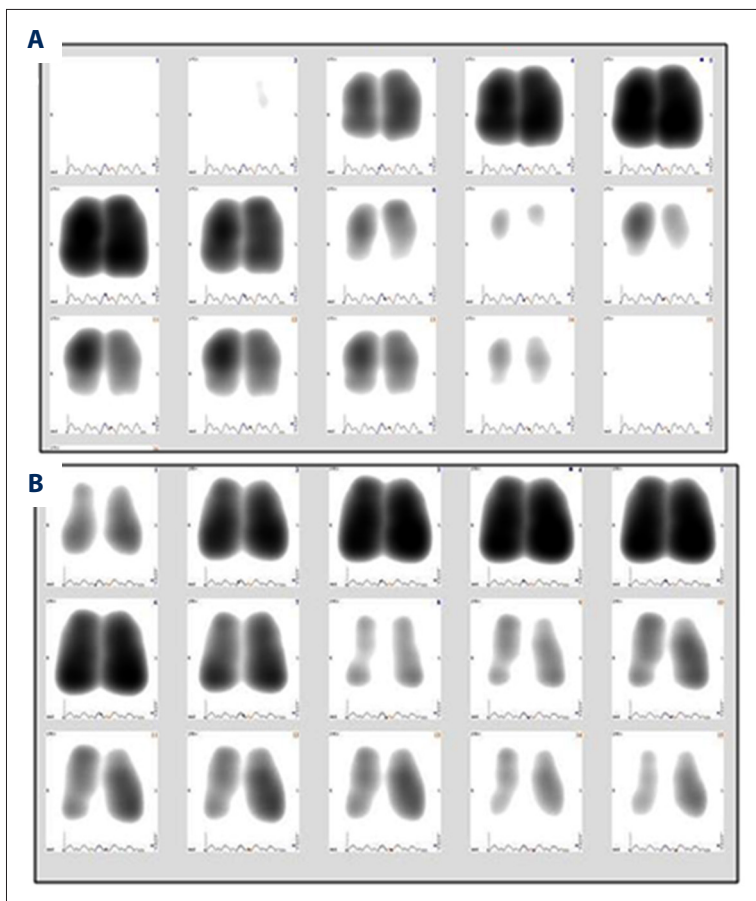


Figure 4. Comparison of residual air at the end of expiratory phase using VRI. (A) (Non-smokers): no residual air at the end of the expiratory phase. (B) (Passive smokers): residual air at the end of the expiratory phase.

and passive smokers. Non-smokers had relatively low residual air at the end of the expiratory phase (25.40%). However, 80.36% and 63.04% of smokers and passive smokers, respectively, had residual air at the end of the expiratory phase. The differences in residual air at the end of the expiratory phase and VRIS between these groups were statistically significant (both $P < 0.001$) (Figures 4, 5).

VRIS

The mean total VRIS of non-smokers was 3.16 ± 1.81 . VRIS of smokers was 6.21 ± 2.03 . VRIS of passive smokers was 5.43 ± 1.87 (all $P < 0.05$).

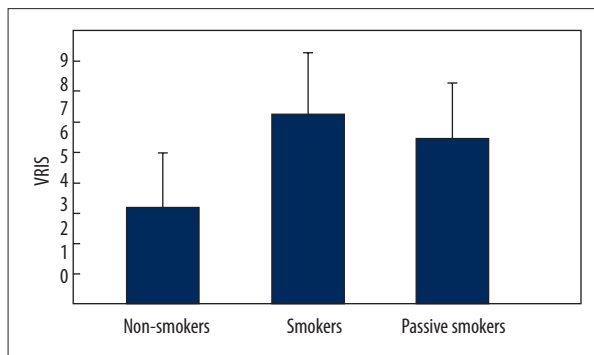


Figure 5. VRIS of non-smokers, smokers, and passive smokers. There were significant differences (all $P = 0.001$) in the VRIS of non-smokers (3.16 ± 1.81), smokers (6.21 ± 2.03) and passive smokers (5.43 ± 1.87).

Table 3. Distribution of quantitative lung data of non-smokers, smokers, and passive smokers.

Lung Region	Non-smokers	Smokers	Passive smokers	p
Total left	55.45±7.29	55.98±8.48	57.87±7.05	0.25
Upper left	10.61±3.18	9.75±2.94	10.65±2.99	0.22
Middle left	20.06±3.67	19.20±3.47	20.83±3.87	0.08
Lower left	24.77±5.08	27.57±6.01	26.83±5.52	0.02*
Total right	44.57±7.23	43.48±7.58	41.91±6.90	0.17
Upper right	7.95±3.21	6.93±2.51	7.00±3.52	0.14
Middle right	14.70±3.44	13.27±3.44	13.59±3.35	0.06
Lower right	21.92±5.05	23.11±4.84	21.33±4.46	0.16

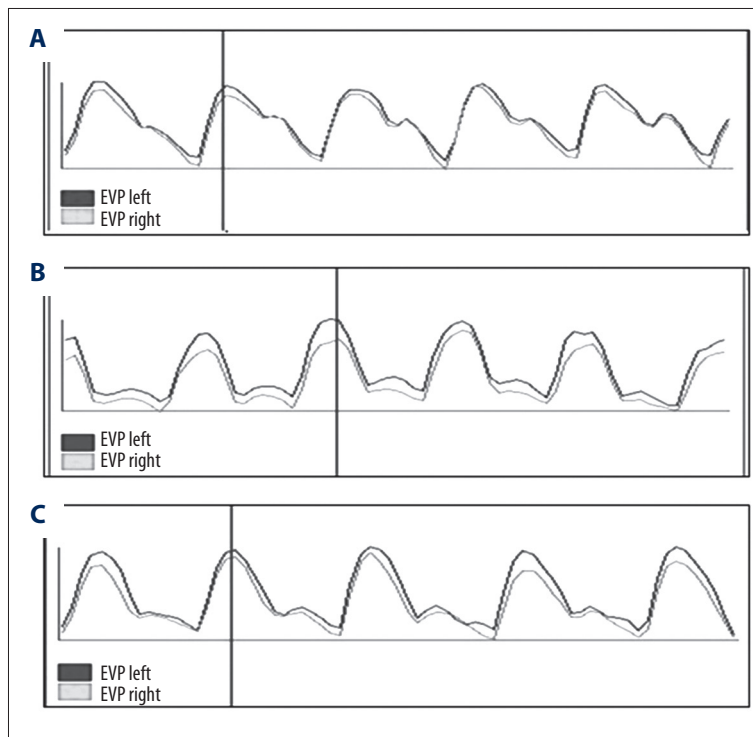


Figure 6. Comparison of EVP (both left and right lung) between smokers and non-smokers. In non-smokers and passive smokers (**A, C**), the amplitudes of EVP between the left and right lungs were almost the same. In smokers (**B**), the amplitudes of EVP between the left and right lungs were different.

Distribution of QLD

Significant differences were found in the distribution of QLD of the left lower lung region between non-smokers and smokers, but not in passive smokers ($P < 0.05$ between non-smokers and smokers) (Table 3).

EVP

The amplitudes of EVP between the left and right lungs were different in smokers and passive smokers, with 55.36% and 58.70%, respectively. However, the difference of amplitudes of EVP between the left and right lungs was relatively lower for non-smokers (22.22%) ($P < 0.05$) (Figure 6).

Correlation between smoking index and VRIS

A weak yet significant relationship was observed between the smoking index and VRIS of smokers and passive smokers ($r = 0.297$; $P = 0.026$) (Figure 7).

Discussion

The aim of the present study was to evaluate the use of VRI and to assess the differences in VRI findings between non-smokers, active smokers and passive smokers. All participants were healthy, with normal X-ray and physical examinations.

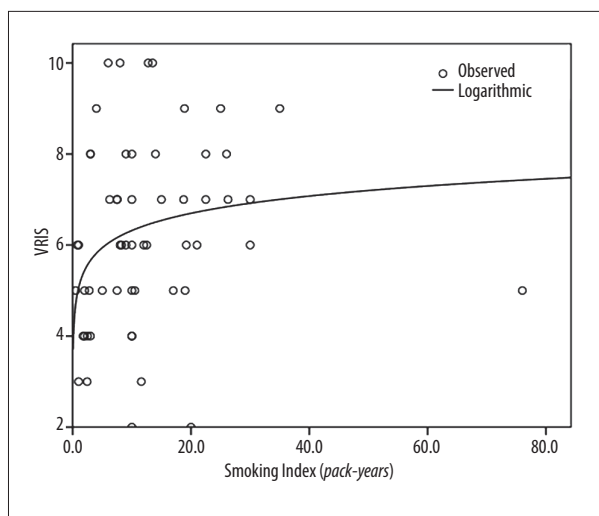


Figure 7. Correlation between the smoking index and VRIS in smokers.

VRI images showed progressive and regressive stages representing the inspiratory and expiratory phases bilaterally in a vertical and synchronized manner in non-smokers. Vibration energy curves with low expiratory phase and plateau were present in 6.35% and 3.17%, respectively, of healthy non-smokers, 41.07% and 28.60% of smokers, and 39.13% and 30.43% of passive smokers. The massive energy peak in the non-smokers, smokers, and passive-smokers was 1.77 ± 0.27 , 1.57 ± 0.29 , and 1.66 ± 0.33 , respectively. A weak but positive association was observed between VRIS and the smoking index.

The characteristics observed in smokers are features of limitation of airflow. Indeed, chronic obstructive pulmonary disease (COPD) is characterized by persistent airflow limitation, and spirometry is required to make the clinical diagnosis of COPD (the presence of a post-bronchodilator $FEV_1/FVC < 0.7$). Smoking is the strongest risk factor of COPD. Pathological characteristic changes of COPD are found in the airways, lung parenchyma, and pulmonary vasculature. Dellinger et al. [1] assessed the role of VRI in evaluating airway obstruction. Increased fibrosis, smooth muscle hypertrophy, inflammation, and increased goblet cells are found in the lungs of healthy smokers who have no known clinical evidence of respiratory disease [13,14]. In the present study, all active and passive smokers had normal spirometric test. However, they had low and plateaued expiratory phase, indicating that tobacco could induce injuries in lungs and airways before the clinical stage of COPD. These histological changes might be subtle. Nevertheless, they alter the transmission of sound vibrations through the airway and lungs, leading to changes visible in the VRI.

MEF can provide more detailed information about respiratory sounds as it reflects air distribution at the peak of air vibration in the lung. Abnormal MEF shapes reflect the air distribution of

regional airway obstruction or stenosis [12]. A previous study has shown an unsmooth edge of MEF image in patients with acute exacerbation of COPD [15]. In the present study, no significant difference was found among non-smokers, smokers, and passive smokers in MEF ($P > 0.05$), which was consistent with the study by Yigla et al. [6]. Both MEF and chest radiography are diagnostic imaging techniques containing air representing the status of the lungs at maximum inspiration. In earlier studies, VRI images were safely used to recognize the location and size of the abnormality through MEF in patients with pneumothorax, pneumonia and pleural effusion [11,16,17]. In the present study, healthy subjects were selected on the basis of history, physical examination and chest X-ray. The chest X-ray results were normal, and correspondingly, there were no differences in MEF between the three groups.

In QLD, the percentage of total breath sound intensity and the average of all 12-second recordings of different regions of the right and left lungs were quantified, which proved complementary to the visual analysis of the images. QLD values were typically higher for the left lung than the right lung, and the energy distribution in the upper lung region was less than half of that in the middle or lower lung region. QLD of the left lower lung in smokers and passive smokers were higher than in non-smokers. The reason is that the left lower bronchus is narrower than the right one, and the airflow transmission through the airway and lung is limited, leading to more workload on the left lower lung. Hence, the distribution of the QLD of the left lower lung region was high. In addition, some major bronchi of the left lung are closer to the posterior chest wall because of the anterior position of the heart [18–20].

In this study, VRIS was calculated by adding up the sub-scores for vibration energy, MEF and dynamic image. Distinct difference in total VRIS was found among non-smokers, active smokers, and passive smokers. Although previous study showed that pack-years of cigarette smoking had a significant negative correlation with left lung QLD, this correlation was not found in the present study. However, a weak positive correlation was found between the smoking index and VRIS, suggesting that more smoking causes more serious damage to the lung, and VRI could show the injury intuitively. In the present study, some young smokers had a low smoking index. However, VRI vibration energy curve showed low and plateaued expiratory phase with high VRIS. These results were consistent with the weak correlation coefficient of 0.297. Earlier studies showed that the detrimental effects of smoking on pulmonary function are greater in women, as compared to those in men, with lung cancer [21]. Consequently, lung damage was associated with the amount of tobacco used, and with the susceptibility to smoking. Moreover, another explanation for the low correlation coefficient is the small number subjects enrolled in the study. A large sample size, especially smokers is

warranted in order to confirm the relationship between smoking index and VRIS.

Tobacco use continues to be the leading global cause of preventable death. Most of these deaths occur in low- and middle-income countries, and this disparity is expected to increase further over the next decades. Cessation of tobacco use can significantly reduce the risk of tobacco-related diseases. However, cessation of tobacco use is difficult and may require multiple attempts. Besides, smokers could not intuitively realize the harms of tobacco use until the development of serious complications. The VRI device (VRIxp, Deep Breeze) was designed for practical clinical applications, displaying breath sounds as static and dynamic gray-scale images. Images from the VRI are visual and intuitive, and if it can reliably distinguish non-smokers from smokers and passive smokers, then they might be used to persuade smokers about tobacco damage. Consequently, a future study of smoking cessation could use this technology.

VRI is a new technology that has numerous advantages, including non-invasiveness and no radiations. Its only contraindications are skin injury on the back, acute respiratory infection, pacemaker or defibrillator, and pregnant or lactating women. As for the indications, any people without these

contraindications may undergo VRI. Therefore, VRI is suitable for a vast array of individuals.

The present study has some limitations. In addition to the small sample size, there was only one female smoker enrolled in this study, while other subjects were male. However, many previous studies have reported the differences in the lung sounds of healthy men and women, and the mechanisms underlying this effect of sex remains to be investigated [4,22,23].

Conclusions

VRI may be used to intuitively show the differences between non-smokers and smokers. VRI revealed that passive smoking can also harm the lungs. VRI could be used to visually persuade smokers to give up smoking. Because of the small sample size and gender imbalance of the present study, further studies are necessary to evaluate the effect of smoking, active or passive, on VRI findings.

Competing interests

All authors declare that they have no competing interests.

References:

1. Dellinger RP, Parrillo JE, Kushnir A et al: Dynamic visualization of lung sounds with a vibration response device: a case series. *Respiration*, 2008; 75: 60–72
2. Anantham D, Herth FJ, Majid A et al: Vibration response imaging in the detection of pleural effusions: a feasibility study. *Respiration*, 2009; 77: 166–72
3. Wang Z, Jean S, Bartter T: Lung sound analysis in the diagnosis of obstructive airway disease. *Respiration*, 2009; 77: 134–38
4. Maher TM, Gat M, Allen D et al: Reproducibility of dynamically represented acoustic lung images from healthy individuals. *Thorax*, 2008; 63: 542–48
5. Yosef M, Langer R, Lev S, Glickman YA: Effect of airflow rate on vibration response imaging in normal lungs. *Open Respir Med J*, 2009; 3: 116–22
6. Yigla M, Gat M, Meyer JJ et al: Vibration response imaging technology in healthy subjects. *Am J Roentgenol*, 2008; 191: 845–52
7. Mineshita M, Shirakawa T, Saji J et al: Vibration response imaging in healthy Japanese subjects. *Respir Investig*, 2014; 52: 28–35
8. World Health Organization. WHO report on reducing risks, promoting healthy life. Geneva: WHO, 2002
9. World Health Organization. WHO report on the global tobacco epidemic. Geneva: WHO, 2011
10. Bing D, Jian K, Long-feng S et al: Vibration response imaging: a novel non-invasive tool for evaluating the initial therapeutic effect of noninvasive positive pressure ventilation in patients with acute exacerbation of chronic obstructive pulmonary disease. *Respir Res*, 2012; 13: 65
11. Blanco M, Mor R, Fraticelli A et al: Distribution of breath sound images in patients with pneumothoraces compared to healthy subjects. Diagnostic yield of vibration response imaging technology. *Respiration*, 2009; 77: 173–78
12. Guntupalli KK, Reddy RM, Loutfi RH et al: Evaluation of obstructive lung disease with vibration response imaging. *J Asthma*, 2008; 45: 923–30
13. Hale KA, Ewing SL, Gosnell BA, Niewoehner DE: Lung disease in long-term cigarette smokers with and without chronic air-flow obstruction. *Am Rev Respir Dis*, 1984; 130: 716–21
14. Cosio Piqueras MG, Cosio MG: Disease of the airways in chronic obstructive pulmonary disease. *Eur Respir J Suppl*, 2011; 34: 41s–49s
15. Holmes JH, Korosec FR, Du J et al: Imaging of lung ventilation and respiratory dynamics in a single ventilation cycle using hyperpolarized He-3 MRI. *J Magn Reson Imaging*, 2007; 26: 630–36
16. Bartziokas K, Daenas C, Preau S et al: Vibration response imaging: evaluation of rater agreement in healthy subjects and subjects with pneumonia. *BMC Med Imaging*, 2010; 10: 6
17. Mor R, Kushnir I, Meyer JJ et al: Breath sound distribution images of patients with pneumonia and pleural effusion. *Respir Care*, 2007; 52: 1753–60
18. Pasterkamp H, Patel S, Wodicka GR: Asymmetry of respiratory sounds and thoracic transmission. *Med Biol Eng Comput*, 1997; 35: 103–6
19. Dosani R, Kraman SS: Lung sound intensity variability in normal men. A contour phonopneumographic study. *Chest*, 1983; 83: 628–31
20. O'Donnell DM, Kraman SS: Vesicular lung sound amplitude mapping by automated flow-gated phonopneumography. *J Appl Physiol Respir Environ Exerc Physiol*, 1982; 53: 603–9
21. Ryu JS, Jeon SH, Kim JS et al: Gender differences in susceptibility to smoking among patients with lung cancer. *Korean J Intern Med*, 2011; 26: 427–31
22. Gross V, Dittmar A, Penzel T et al: The relationship between normal lung sounds, age, and gender. *Am J Respir Crit Care Med*, 2000; 162: 905–9
23. Bellemare F, Jeanneret A, Couture J: Sex differences in thoracic dimensions and configuration. *Am J Respir Crit Care Med*, 2003; 168: 305–12